

closely similar (Scheme IV). Whichever mechanistic classification may be followed, the reaction must involve $3^{++}/2$, given the gross difference in ionization potentials and the difficulty of ionizing **2**. The $[3 + 2]$ reaction could produce two diastereoisomeric adducts (**7a,b**), while the $[4 + 1]$ cycloaddition should produce a single diastereoisomer (**8**). In fact, both the aminium salt initiated and photosensitized cross additions of **2** and **3** produce all three isomers in the ratios **7a**:**7b**:**8** = 0.5:0.7:1.0. The $[3 + 2]$: $[4 + 1]$ ratio is therefore 1.2:1.

The assumption that the more readily ionized diene is the hole-carrying species in these reaction systems can be justified quantitatively. The rate constant for the cyclodimerization $1^{++}/1$ has been measured ($3 \times 10^8 \text{ mol L}^{-1} \text{ s}^{-1}$).⁹ The analogous reaction $1^{++}/2$ is estimated to have a rate constant of at least 1.5×10^8 on the basis that even the relatively more stabilized (more selective) *trans*-anethole cation radical adds (in the Diels-Alder mode) to **1** and **2** at the relative rate of only 2:1. A species of higher hole energy, such as 1^{++} , would be presumed to react with **1** and **2** even less selectively. The corresponding role-inverted reaction $2^{++}/1$ requires the generation of 2^{++} , which is qualitatively indicated to be quite difficult by the observation that **2** is essentially inert under the aminium salt conditions. Given the measured oxidation potentials of **1**, **2**, and **3**, the rate of generation of 2^{++} must be a factor of 10^5 slower than the rate of generation of 1^{++} at 0 °C.¹⁰ For the overall rate of the $2^{++}/1$ reaction to compete with that of the $1^{++}/2$ reaction, the rate constant for the cycloaddition $2^{++}/1$ would then have to be at least 10^{13} , or 10^3 faster than the maximum diffusion-controlled rate. In the case of the $2^{++}/3$ reaction, the even larger difference in ionization potentials (0.49 V) and the correspondingly greater ratio of the rates of formation of 3^{++} relative to 2^{++} (10^7) would require a $2^{++}/3$ cycloaddition rate of 10^{15} . The virtual absence of the dimer of **2** as a product of any of these reactions also independently supports the proposed mechanistic role assignments. Since 2^{++} has high hole energy and is not sterically stabilized, its reactions with **2** vs **1** or **3** should be quite rapid and unselective. The amount of dimer formation is therefore an approximate measure of the amount of cross adduct formed via the $2^{++}/1$ or **3** mechanism.

These studies suggest that orbital symmetry allowedness/forbiddenness has no discernible effect on role selectivity in the cation radical Diels-Alder reaction. Although the factors that determine adduct selectivity are not as yet completely defined, they appear to correlate with product development control (e.g., adduct strain energies) and to vanish for adduct structures that are quite similar. The apparent irrelevance of orbital symmetry effects is consistent with the facility of such formally symmetry forbidden cation radical reactions as cyclobutane (*S/S* stereochemistry) and the cation radical vinylcyclobutane rearrangement (*S/R* stereochemistry). The failure of orbital symmetry to exert even a small effect on role selectivity is interesting theoretically, and the following factors may be involved: (i) activation energies for cation radical cycloadditions generally are miniscule in comparison with neutral cycloadditions; differential effects may thus be vanishingly small; (ii) cation radical cycloadditions are highly nonsynchronous; orbital symmetry effects on such reactions should be minimal.

Acknowledgment. We thank the National Science Foundation (CHE-8822051) for support of this research.

Supplementary Material Available: Experimental details for the cycloaddition reactions of **1** and **2**, **1** and **3**, and **2** and **3** by both the aminium salt procedure and the photosensitized electron-transfer procedure (3 pages). Ordering information is given on any current masthead page.

(9) Calhoun, G. C.; Schuster, G. B. *J. Am. Chem. Soc.* **1984**, *106*, 6870.

(10) From the Marcus equation, $\Delta G^\ddagger = \Delta G_0^\ddagger(1 + \Delta G_0^\ddagger/4\Delta G_0^\ddagger)^2$, using $\Delta G_0^\ddagger = 7 \text{ kcal/mol}$ and ΔG_0^\ddagger from the difference in oxidation potentials of **4** (1.05 V) and the appropriate diene (1.85, 1.53, 1.36 V). The above value of ΔG_0^\ddagger was experimentally derived for the aminium salt/diene endoergic hole transfers and is in accord with other measurements.^{11,12}

(11) Schlessener, C. J.; Amatore, C.; Kochi, J. K. *J. Am. Chem. Soc.* **1984**, *106*, 3567-77.

(12) Johnson, M. D.; Miller, J. R.; Green, N. D.; Closs, G. L. *J. Phys. Chem.* **1989**, *93*, 1173.

Synthesis, Structure, and Magnetic Properties of the Stable Triangular $[\text{Mn}^{\text{IV}}_3\text{O}_4]^{4+}$ Core

N. Auger and J.-J. Girerd*

UA CNRS 420, Institut de Chimie Moléculaire
Université de Paris-Sud, 91405 Orsay, France

M. Corbella

Dpt de Quimica Inorganica, Facultat de Quimica
Universitat de Barcelona, Diagonal 647
08028 Barcelona, Spain

A. Gleizes

Laboratoire de Chimie de Coordination du CNRS
31077 Toulouse, France

J.-L. Zimmermann

Service de Biophysique, Département de Biologie
CEN-Saclay, 91191 Gif-sur-Yvette Cedex, France
Received July 17, 1989

The structure of the oxygen evolving center (OEC) in photosystem II of plants and the mechanism of water oxidation are still unknown. Recent biological results have been reviewed in ref 1. Chemists can contribute to this study by synthesizing new manganese clusters and studying the electronic properties of those complexes; then useful comparisons can be made with the spectroscopic properties of the natural system. This approach led, for instance, to the synthesis of $[\text{Mn}_4\text{O}_3\text{Cl}]^{6+}$ cores^{2,3} and of adamantane-like $[\text{Mn}_4\text{O}_6]^{4+}$ cores.^{4,5} Chemical results have been reviewed in ref 6. We report here the synthesis and magnetic studies of a new type of manganese cluster made of a triangular $[\text{Mn}_3\text{O}_4]^{4+}$ core with two mono- μ -oxo bridges and one di- μ -oxo bridge.

Synthesis was carried out under argon. A solution of MnCl_2 (1.8 mmol) in 4 mL of DMF¹⁰ and a solution of bipy (4 mmol) and TsOH (3.2 mmol) in 4 mL of DMF were mixed. Before any precipitate appeared, this solution was added to a solution of NEt_4MnO_4 (1.2 mmol) in 8 mL of DMF; a dark brown solution was obtained. After 16 h, addition of $(\text{NEt}_4)_2\text{MCl}_4$ (1 mmol) ($M = \text{Mn}$ or Cd) in 14 mL of DMF afforded brown powders of stoichiometry $[\text{Mn}_3\text{O}_4(\text{bipy})_4\text{Cl}_2]\text{MCl}_4 \cdot 3\text{DMF}$ after washing with acetonitrile ($M = \text{Mn}$ (**1**), Cd (**2**)).⁷ Crystals of **1** were obtained

(1) Brudvig, G. W.; Beck, W. F.; de Paula, J. C. *Annu. Rev. Biophys. Biophys. Chem.* **1989**, *18*, 25-46.

(2) Bashkin, J. S.; Chang, H.-R.; Streib, W. E.; Huffman, J. C.; Hendrickson, D. N.; Christou, G. *J. Am. Chem. Soc.* **1987**, *109*, 6502-6504.

(3) (a) Christou, G.; Vincent, J. B. *Biochim. Biophys. Acta* **1987**, *895*, 259-274. (b) Li, Q.; Vincent, J. B.; Libby, E.; Chang, H.-R.; Huffman, J. C.; Boyd, P. D. W.; Christou, G.; Hendrickson, D. N. *Angew. Chem., Int. Ed. Engl.* **1988**, *27*, 1731-1733.

(4) (a) Wieghardt, K.; Bossek, U.; Gebert, W. *Angew. Chem., Int. Ed. Engl.* **1983**, *22*, 328-329. (b) Wieghardt, K.; Bossek, U.; Nuber, B.; Weiss, J.; Bonvoisin, J.; Corbella, M.; Vitols, S.; Girerd, J.-J. *J. Am. Chem. Soc.* **1988**, *110*, 7398-7411.

(5) Hagen, K. S.; Westmoreland, T. D.; Scott, M. J.; Armstrong, W. H. *J. Am. Chem. Soc.* **1989**, *111*, 1907-1909.

(6) Pecoraro, V. L. *Photochem. Photobiol.* **1988**, *48*, 249-264.

(7) Anal. Calcd for **1** ($\text{C}_{49}\text{H}_{53}\text{Cl}_2\text{Mn}_3\text{N}_4\text{O}_7$): C, 43.90; H, 3.99; N, 11.49; Cl, 15.87; Mn, 16.39. Found: C, 42.91; H, 3.83; N, 11.1; Cl, 16.51; Mn, 16.19. Anal. Calcd for **2** ($\text{C}_{49}\text{H}_{53}\text{CdMn}_3\text{Cl}_2\text{N}_4\text{O}_7$): C, 42.10; H, 3.82; N, 11.02; Cl, 15.21; Mn, 11.79; Cd, 8.04. Found: C, 41.83; H, 3.55; N, 10.72; Cl, 15.11; Mn, 11.43; Cd, 7.75. Yield around 60% based on bipy.

(8) X-ray analysis of **1**: orthorhombic, space group *Pbca*, $a = 17.137$ (3) Å, $b = 23.917$ (5) Å, $c = 27.786$ (7) Å, $V = 11388$ Å³, $Z = 8$; $R = 0.070$ for 319 variables and 2644 observed [$I > 2\sigma(I)$] diffractometer-collected reflections (Mo $K\alpha$ radiation, 293 K). The DMF molecules were found disordered, and the disorder could not be solved. Difference-Fourier peaks not inconsistent with solvent molecule atoms were introduced in calculations as statistically distributed C atoms with partial site occupancies (atoms C(d) in table of positional parameters in supplementary material).

(9) George, G. N.; Prince, R. C.; Cramer, S. P. *Science* **1989**, *243*, 789-791. See also: Yachandra, V. K.; Guiles, R. D.; McDermott, A. E.; Cole, J. L.; Britt, R. D.; Dexheimer, S. L.; Sauer, K.; Klein, M. P. *Biochemistry* **1987**, *26*, 5974-5981.

(10) Abbreviations used: DMF = dimethylformamide, TsOH = *p*-toluenesulfonic acid, NEt_4^+ = tetraethylammonium cation, bipy = bipyridine, OEC = oxygen evolving center, EPR = electron paramagnetic resonance, zFS = zero-field splitting.

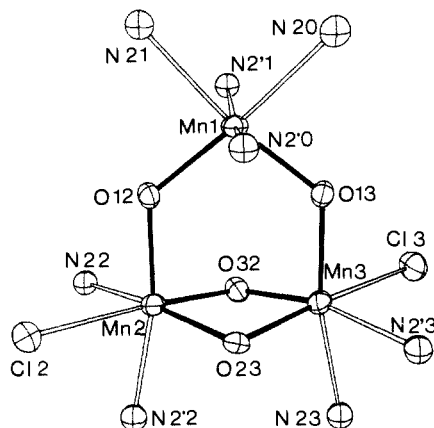


Figure 1. Structure of $[\text{Mn}_3\text{O}_4(\text{bipy})_4\text{Cl}_2]^{2+}$ showing atom-labeling scheme (only the N atoms of bipy are shown). Selected interatomic distances (angstroms) and angles (degrees): Mn(1)–O(12), 1.758 (9); Mn(1)–O(13), 1.766 (9); Mn(2)–O(12), 1.833 (10); Mn(2)–O(32), 1.834 (10); Mn(2)–O(23), 1.809 (9); Mn(2)–Cl(2), 2.330 (5); Mn(3)–O(13), 1.833 (10); Mn(3)–O(32), 1.785 (10); Mn(3)–O(23), 1.849 (9); Mn(3)–Cl(3), 2.343 (5); Mn(1)–O(12)–Mn(2), 128.9 (5); Mn(1)–O(13)–Mn(3), 128.7 (5); Mn(2)–O(32)–Mn(3), 95.6 (4); Mn(2)–O(23)–Mn(3), 94.3 (4).

in DMF. The crystal structure of **1** was determined.⁸

The structure is made of trinuclear cationic entities $[\text{Mn}_3\text{O}_4(\text{bipy})_4\text{Cl}_2]^{2+}$ (see Figure 1) with tetrahedral $[\text{MnCl}_4]^{2-}$ as counterions. The Mn atoms of the cations occupy the corners of an isosceles triangle: Mn(1)–Mn(2) = 3.241 (3) Å, Mn(1)–Mn(3) = 3.245 (3) Å, and Mn(2)–Mn(3) = 2.681 (3) Å. Two single oxo bridges relate Mn(1) to Mn(2) and Mn(3), while Mn(2) and Mn(3) are linked by a double oxo bridge. The single-bridge O(12) and O(13) atoms are in the plane of the triangle, while the double-bridge O(23) and O(32) atoms form a segment perpendicular to it. The dihedral angle along O(23)–O(32) is equal to 16.2 (8)°. The manganese coordinations are octahedrally completed by four bipyridine N atoms for Mn(1) and by two bipyridine N atoms and one Cl atom for Mn(2) and Mn(3). Both analysis and crystal structure demonstrate that the cluster contains three Mn(IV) ions. The metal–metal distances correspond to those observed in the OEC⁹ in the S_1 state.¹¹ Compound **2** is isomorphous to compound **1**.

Measurement of the magnetic susceptibility was done for **1** and **2**. The results for **2** are shown in Figure 2. The product $\chi_M T$ per mole of **2** is equal to 1.79 $\text{cm}^3 \text{mol}^{-1} \text{K}$ at 293.2 K and decreases to 0.37 $\text{cm}^3 \text{mol}^{-1} \text{K}$ at 3.9 K. This behavior is characteristic of strong antiferromagnetic coupling between the electronic spins of the three metallic ions leading to a spin $S = 1/2$ ground state. The product $\chi_M T$ per mole of **1** is equal to 6.16 $\text{cm}^3 \text{mol}^{-1} \text{K}$ at 292.1 K and decreases to 4.79 $\text{cm}^3 \text{mol}^{-1} \text{K}$ at 3.8 K. At high temperature, $\chi_M T$ of **1** is exactly the sum of $\chi_M T$ of **2** and 4.375 $\text{cm}^3 \text{mol}^{-1} \text{K}$, which is the value associated with the spin $S = 5/2$ of the MnCl_4^{2-} anion. At lower temperature, some nonadditivity appeared, which was reproducible and which we attributed to an interaction between the cluster spin and the counteranion spin. We analyzed only the data for **2**. Using a Hamiltonian of the type

$$H = -J'(S_1 S_2 + S_1 S_3) - JS_2 S_3 \quad (1)$$

a good fit (Figure 2) was found with $J = -171 \text{ cm}^{-1}$ and $J' = -108 \text{ cm}^{-1}$, keeping g fixed at 2. The ground state is thus $|S_{23} = 1, S_1 = 3/2, S = 1/2\rangle$.

The EPR spectrum of **2** was recorded in water at 7.7 K in the presence of glycerol (Figure 3). The richness of its hyperfine structure is by itself an indication that the cluster is maintained in aqueous solution. More precisely, we interpreted the spectrum from the ground state observed in the solid sample. Calculation

(11) S_1 or S_2 refers here to one of the five states of the OEC and not to a spin value; see, for instance, ref 1 for an introduction to this nomenclature.

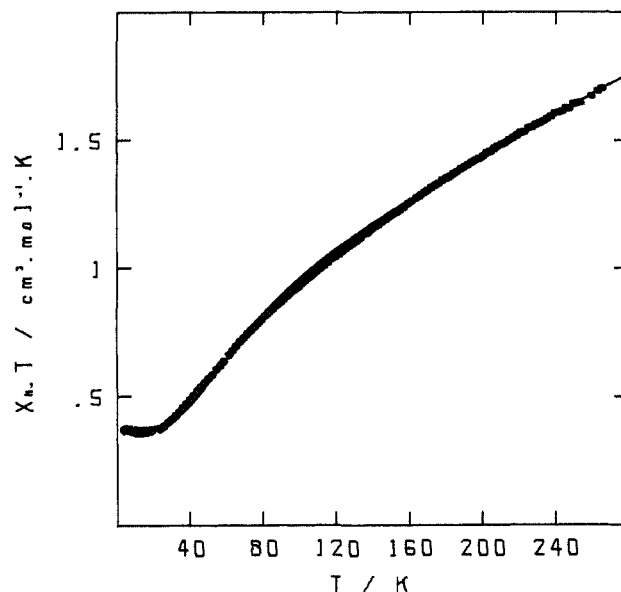


Figure 2. Powder magnetic susceptibility of **2** (\diamond) under the form $\chi_M T$ versus temperature. The line corresponds to the fitting (see text) with $J_{23} = J = -171 \text{ cm}^{-1}$ and $J_{12} = J_{13} = J' = -108 \text{ cm}^{-1}$. The ground state is a spin doublet.

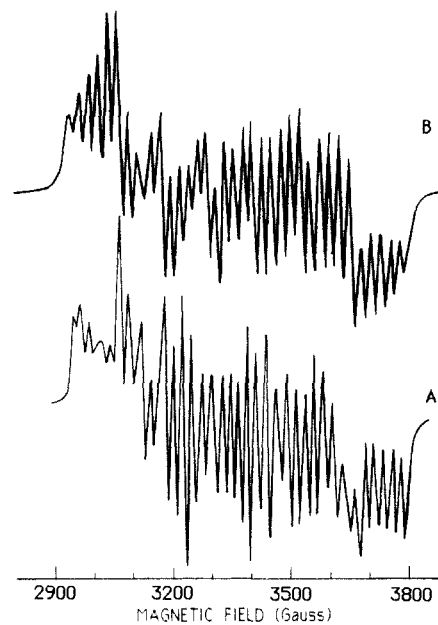


Figure 3. (A) X-band EPR spectrum of **2** in water +20% glycerol at 7.7 K. (B) Simulation using $|A_{1x,y}| = 118 \text{ G}$, $|A_{1z}| = 121 \text{ G}$, $|A_{2x,y}| = 26 \text{ G}$, $|A_{2z}| = 24 \text{ G}$, $|A_{3x,y}| = 25 \text{ G}$, $|A_{3z}| = 22 \text{ G}$, $g_{x,y} = 2$, and $g_z = 1.995$; line width = 17 G.

of the hyperfine constants for the ground state $|S_{23} = 1, S_1 = 3/2, S = 1/2\rangle$ gives $A_2 = A_3 = -(1/3)a$ and $A_1 = (5/3)a$, where a stands for the mononuclear value of the hyperfine coupling for a Mn(IV) ion. Simulation of the spectrum affords the values $|A_{1x,y}| = 118 \text{ G}$, $|A_{1z}| = 121 \text{ G}$, $|A_{2x,y}| = 26 \text{ G}$, $|A_{2z}| = 24 \text{ G}$, $|A_{3x,y}| = 25 \text{ G}$, $|A_{3z}| = 22 \text{ G}$, $g_{x,y} = 2$, and $g_z = 1.995$. With $a = 72 \text{ G}$, the $|S_{23} = 1, S_1 = 3/2, S = 1/2\rangle$ wave function gives $A_2 = A_3 = -24 \text{ G}$ and $A_1 = 120 \text{ G}$, which are very close to the values got by simulation. The EPR simulation suggests a slight dissymmetry in solution between site 2 and site 3 which is beyond the sensitivity of powder magnetic susceptibility measurement. A $|S_{23} = 2, S_1 = 3/2, S = 1/2\rangle$ ground state (which is the only other spin doublet eigenfunction of eq 1) would lead to $A_2 = A_3 = a$ and $A_1 = -a$; no simulation of the observed spectrum was possible with such values, which confirms our analysis of magnetic data.

The possibility of interpreting the EPR spectrum of a spin $S = 1/2$ state resulting from the magnetic coupling of the manganese

atoms in the core $[\text{Mn}_3\text{O}_4]^{4+}$, using the spin coupling model without the zero-field splitting (zFS) effect, is noteworthy: J values are so large that the ground state is a real spin doublet. There is general agreement^{12,14,15} on a $S = 1/2$ origin of the multiline EPR signal observed for the S_2 state¹¹ of the OEC. A detailed study¹³ showed that the g -anisotropy of this signal was very small and proved the $S = 1/2$ nature of the state implied. Recently¹⁶ it was demonstrated that anisotropy in the OEC signal arises from anisotropy in the hyperfine coupling. Our result strongly suggests that this OEC signal could be interpreted on the basis of spin coupling as suggested earlier by some authors^{14,15} with anisotropic effects treated as perturbation only. We are working on simulations of the OEC signal along those lines.

A cubane-type structure of the OEC was proposed by Brudvig¹² and Christou,^{2,3} a distorted cubane structure and a structure made of a manganese triangle linked to a manganese atom were proposed recently⁹ for the S_1 state. Such a 3 + 1 structure of the copper cluster in ascorbate oxidase (which catalyzes the reverse reaction of OEC) was found through X-ray diffraction by Huber,¹⁷ who also proposed that the OEC could have a 3 + 1 arrangement of the manganese atoms. Our result shows that manganese-oxo triangular units exist. We are investigating the possibility of assembling this Mn(IV)_3 entity with a Mn(III) ion.

Acknowledgment. M.C. has benefited from a grant from Spain and CNRS (France).

Supplementary Material Available: Tables of positional parameters for non-H and H atoms, anisotropic and isotropic thermal parameters, and main interatomic distances and angles for **1** (6 pages); table of observed and calculated structure factors for **1** (13 pages). Ordering information is given on any current masthead page.

(12) de Paula, J. C.; Beck, W. F.; Brudvig, G. W. *J. Am. Chem. Soc.* **1986**, *108*, 4002-4009.

(13) Hansson, O.; Aasa, R.; Vanngard, T. *Biophys. J.* **1987**, *51*, 825-832.

(14) Dismukes, G. C.; Siderer, Y. *Proc. Natl. Acad. Sci. U.S.A.* **1981**, *78*, 274-278.

(15) Hansson, O.; Andréasson, L.-E. *Biochim. Biophys. Acta* **1982**, *679*, 261-268.

(16) Haddy, A.; Aasa, R.; Andréasson, L.-E. *Biochemistry* **1989**, *28*, 6954-6959.

(17) Huber, R. *Angew. Chem., Int. Ed. Engl.* **1989**, *28*, 848-869.

Diastereoselective Reduction of 9-Oxo-13-tetradecanolide and 10,10-Dimethyl-9-oxo-13-tetradecanolide

Thomas H. Keller[†] and Larry Weiler*

The University of British Columbia
Department of Chemistry, 2036 Main Mall
Vancouver, British Columbia, Canada V6T 1Y6

Received May 15, 1989

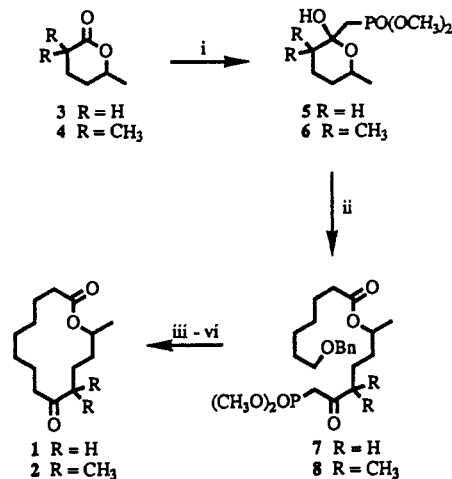
In 1981 Still and Galynker^{1a} reported the stereoselective alkylations of a number of monosubstituted 8-12-membered-ring ketones and lactones. Invariably these reactions proceeded with high selectivity, to yield one of the two possible diastereomeric products. In order to rationalize the high diastereoselectivity of these reactions, Still and co-workers¹ used MM2 calculations.² The model that emerged from these studies¹ assumed that attack of a reagent from the more open face of the macrocycle gave rise to product ratios that were closely related to the conformational

[†] Present address: The University of Toronto, Department of Chemistry, Toronto, Ontario, Canada M5S 1A1.

(1) (a) Still, W. C.; Galynker, I. *Tetrahedron* **1981**, *37*, 3981. (b) Still, W. C.; MacPherson, L. J.; Harada, T.; Callahan, J. F.; Rheingold, A. L. *Tetrahedron* **1984**, *40*, 2275. (c) Still, W. C. *Curr. Trends Org. Synth., Proc. Int. Conf. 4th* **1983**, 233.

(2) Burkert, U.; Allinger, N. L. *Molecular Mechanics*; ACS Monograph 177, American Chemical Society: Washington, DC, 1982.

Scheme I^a



^a (i) $\text{CH}_3\text{PO}(\text{OCH}_3)_2$, 2 equiv of BuLi, THF, -78°C ; (ii) $\text{BnO}(\text{CH}_2)_6\text{COOH}$, DCC, DMAP, DMF; (iii) H_2 , 10% Pd/C, EtOH; (iv) DCC, DMSO, Cl_2HCCOOH ; (v) K_2CO_3 , 18-crown-6, toluene; (vi) H_2 , 10% Pd/C, EtOH.

Table I. Reduction of 9-Oxo-13-tetradecanolide (**1**) with Various Reducing Agents

reducing agent	yield, %	temp, °C	stereoselectivity	
			9 (R^*, S^*)	10 (S^*, S^*)
NaBH_4	89	-78	50	50
K-Selectride	89	-78	78	22
L-Selectride	85	0	80	20
L-Selectride	93	-78	89	11
LS-Selectride	85	-78	90	10
predicted selectivity (MM2)		-78	94	6
MAD	63	-78	30	70

energies of the starting materials or intermediates (for an early transition state) or to the products themselves (for a late transition state).

More recently, a slightly different approach was used to rationalize the diastereoselective reactions of cyclodecenes. Vedejs and co-workers³ eliminated the need for a full conformational analysis of the starting material or product by concentrating only on the immediate environment of the functional group. This local conformer approach has been very successful in rationalizing conformationally controlled epoxidations and osmylations.

We have been interested in studying the reactivity of 14-membered lactones⁴ with the hope of developing a model^{4c} to rationalize and eventually predict the stereoselective reactions in these ring systems. This communication reports our results on the reductions and conformational properties of 9-oxo-13-tetradecanolide (**1**) and 10,10-dimethyl-9-oxo-13-tetradecanolide (**2**).

Our starting materials for this study, macrolides **1** and **2**, were synthesized in 22% and 20% overall yields, respectively, starting from lactones **3**⁵ and **4**, by the sequence outlined in Scheme I.⁶ δ -Lactone **4** is available from 2,2-dimethyl-5-oxohexanoic acid⁷ through sodium borohydride reduction.

(3) (a) Vedejs, E.; Gapinski, D. M. *J. Am. Chem. Soc.* **1983**, *105*, 5058. (b) Vedejs, E.; Dolphin, J. M.; Gapinski, D. M.; Mastalerz, H. *Curr. Trends Org. Synth., Proc. Int. Conf., 4th* **1983**, 221. (c) Vedejs, E.; Dent, W. H.; Gapinski, D. M.; McClure, C. K. *J. Am. Chem. Soc.* **1987**, *109*, 5437.

(4) (a) Neeland, E. G.; Ounsworth, J. P.; Sims, R. J.; Weiler, L. *Tetrahedron Lett.* **1987**, *28*, 35. (b) Ferreira, J. T. B.; Neeland, E. G.; Ounsworth, J. P.; Weiler, L. *Can. J. Chem.* **1987**, *65*, 2314. (c) Keller, T. H.; Neeland, E. G.; Rettig, S.; Trotter, J.; Weiler, L. *J. Am. Chem. Soc.* **1988**, *110*, 7858. (d) Keller, T. H. Ph.D. Thesis, University of British Columbia, June 1988.

(5) Ansell, M. E.; Emmet, J. C.; Coombs, R. V. *J. Chem. Soc. C* **1968**, 217.

(6) All new compounds have been fully characterized spectroscopically and the elemental compositions established by microanalysis or high-resolution mass spectrometry.

(7) Cella, J. A. *Synth. Commun.* **1983**, *13*, 93.